

Stabilization of spatiotemporally chaotic semiconductor laser arrays by means of delayed optical feedback

M. Münkel and F. Kaiser

*Darmstadt University of Technology, Institute for Applied Physics-Nonlinear Dynamics, Hochschulstrasse 4a,
64289 Darmstadt, Germany*

O. Hess

Institute for Technical Physics, DLR, Pfaffenwaldring 38-40, 70569 Stuttgart, Germany

(Received 14 May 1997)

A stabilization scheme for suppression of spatiotemporal instabilities in semiconductor laser arrays is presented. Using relevant time scales obtained from an application of a complex Karhunen-Loève decomposition allows tailoring delayed optical feedback such that stabilization is achieved via destructive interference in the higher-order transverse modes conveying the instabilities. Successful stabilization of previously spatiotemporally chaotic optical near fields towards stable continuous wave output is demonstrated in two-, three- and five-stripe arrays. Linear stability analysis of a system of ordinary differential equations obtained by projection onto the relevant eigenmodes of the two-stripe laser shows that stabilization can be achieved in a wide parameter range. Our analytical results are in good agreement with numerical simulations.

[S1063-651X(97)00510-2]

PACS number(s): 05.45.+b, 42.65.Sf, 42.55.Px

I. INTRODUCTION

The enormous technical progress and the extreme versatility of semiconductor lasers has lead to an ever increasing importance of these devices in many present and future key technologies, e.g., telecommunications, consumer electronics, or manufacturing. To this day, however, a limiting factor resides in the fact that temporal and spatiotemporal instabilities can arise under typical operating conditions desired for applications. Due to its very high gain and outcoupling rate, the semiconductor laser is very sensitive to delayed optical feedback caused by distant reflecting surfaces such as a compact disk or a fiber butt end. An early theoretical investigation of the nonlinear dynamical phenomena resulting from a feedback-induced destabilization was carried out by Lang and Kobayashi more than 15 years ago [1], who described the laser by delay-differential rate equations. In both experimental and theoretical investigations [2,3] it was found that very small amounts of delayed optical feedback can be sufficient to drive the laser into the so-called coherence-collapse regime [4] where the laser output displays irregular behavior with an extremely broadened spectral line. Mørk *et al.* [3] found that this state corresponds to deterministic chaos. On the other hand, it is possible to achieve improved longitudinal mode selection and considerable linewidth narrowing by deliberately applying delayed optical feedback. Moreover, controlling chaos in a semiconductor laser by means of delayed optical feedback [5] and stabilization of traveling waves by means of delayed optical feedback and spatial filtering in a broad-area laser model [6] were demonstrated in recent theoretical works.

Another destabilizing mechanism is closely related to the nonlinear interaction of multiple transverse modes. In multi-stripe and broad area lasers, which are used to obtain very high intensities, these transverse modes become excited

when the pump current exceeds a certain threshold. Then a both temporally and spatially irregular behavior corresponding to deterministic spatiotemporal chaos is observed [7–9], even in the longitudinal single-mode case. This constitutes a severe problem when good beam quality at high intensities is desired. While theoretical investigations of delay-induced temporal instabilities in single-stripe lasers using the Lang-Kobayashi rate equations has been a subject of intense research until today, the investigation of spatiotemporal phenomena occurring in multistripe laser arrays [7,10,11] and broad-area lasers [8,12] has evolved to an issue of great interest in recent years. In recent theoretical work of the authors [13] and other groups [14], both destabilizing mechanisms were combined in investigations on the influence of delayed optical feedback on spatiotemporal dynamics.

In this paper we apply delayed optical feedback to achieve suppression of spatiotemporal instabilities. Thus we can stabilize stationary operation in the fundamental transverse mode from an originally spatiotemporally chaotic state. In Sec. II we will give a brief survey of our model. In Sec. III we introduce complex eigenmode analysis via the Karhunen-Loève algorithm, which yields a decomposition of the complex optical field into a set of orthonormal transverse modes and the individual oscillation frequencies of these modes. Section IV shows that this permits setting up optical feedback conditions that lead to steady-state operation in the fundamental transverse mode by suppression of higher-order transverse modes. By projection onto the relevant eigenmodes we obtain for the case of the two-stripe laser a system of coupled ordinary-differential equations (ODEs) that allows us to perform a linear stability analysis of the fundamental mode (Sec. IV C). Our analytical results are in good agreement with numerical simulations and in Sec. IV D the extension of the stabilization scheme to three- and five-stripe laser arrays is demonstrated.

II. MODEL EQUATIONS

For numerical simulations, we extended the plane-wave Lang-Kobayashi model [1] to include transverse effects. These arise, on the one hand, by transverse coupling via optical diffraction (diffraction coefficient D_p) and charge carrier diffusion (D_f) and, on the other hand, by the transverse inhomogeneity of stripe-geometry lasers. We thus obtain the following set of nonlinear coupled partial differential equations (PDEs) for the complex optical field $E(x,t)$ and the charge carrier density $N(x,t)$:

$$\begin{aligned} \frac{n_l}{c} \partial_t E &= iD_p \partial_x^2 E - [\gamma_E + i\eta(x)]E \\ &+ \Gamma(x)[g(N) + ik_0 \delta n(N)]E \\ &+ \frac{1}{2L} \gamma_R e^{i\Phi} E(x, t - \tau), \end{aligned} \quad (1)$$

$$\partial_t N = \Lambda(x) + D_f \partial_x^2 N - \gamma_{nr} N - \frac{2\epsilon_0 c}{\hbar \omega_0 n_l} g(N) |E|^2. \quad (2)$$

The transversely varying parameters $\Lambda(x)$, $\eta(x)$, and $\Gamma(x)$ describe current injection via stripe electrodes of a given width w and spacing s , index guiding through transverse index steps located below the stripe electrodes, and the transversely varying confinement factor, respectively [13]. Further parameters are the nonradiative decay rate γ_{nr} of the carrier density, the refractive index of the active layer n_l , and the carrier frequency and vacuum wave number ω_0 and k_0 , respectively. The variation of the optical gain and the refractive index of the active medium with the carrier density is approximated by the phenomenological linear gain function $g(N) = a(N - N_0)$ (a is the linear gain coefficient and N_0 the carrier density at transparency) and $\delta n = -\alpha a N / k_0$, respectively [15]. The linewidth enhancement factor is assumed as $\alpha = 2$.

The distributed mirror loss is represented by the damping constant $\gamma_E = -\ln \sqrt{R_1 R_2} / 2L$, where R_1 and R_2 are the power reflectivities of the front and rear facets, respectively. Delayed optical feedback is represented by the feedback parameters γ_R (feedback strength), τ (delay time), and Φ (feedback phase), respectively. The values of relevant parameters are given in Table I. Equations (1) and (2) are solved using a Hopscotch method, assuming absorbing boundary conditions at the transverse edges [16].

III. EIGENMODE ANALYSIS

In order to characterize the spatiotemporal complexity in the laser output, it is highly desirable to find out how many optical modes are involved and the way they are spatially structured. To this end, eigenmode analysis via Karhunen-Loève decomposition (KLD) has been successfully applied in recent publications [17–19]. Given a time series of a spatially extended system (from experiment or numerical simulation), this method provides a decomposition into an orthonormal set of eigenmodes. In its original form, this algorithm computes eigenmodes for real input data. In optics one therefore generally uses data of the output intensity. On this basis, however, the structure of the complex field modes and their

TABLE I. Parameters of the semiconductor laser.

$L = 250 \mu\text{m}$	cavity length
$w = 5.0 \mu\text{m}$	stripe width
$s = 6.0 \mu\text{m}$	stripe separation
$d = 0.15 \mu\text{m}$	thickness of active layer
$R_1 = 0.32$	power reflectivity of the front facet
$R_2 = 0.99$	power reflectivity of the rear facet
$\lambda = 815 \text{ nm}$	laser wavelength
$n_l = 3.59$	refractive index of active layer
$n_c = 3.32$	refractive index of cladding layer
$a = 1.5 \times 10^{-16} \text{ cm}^2$	linear gain coefficient
$b = -1.0 \times 10^2 \text{ cm}^{-1}$	linear loss coefficient
$D_p = 18 \times 10^{-9} \text{ m}$	diffraction coefficient
$\gamma_{nr} = 2 \times 10^8 \text{ s}^{-1}$	nonradiative recombination coefficient
$\Gamma = 0.5014$	confinement factor below stripes
$\Gamma = 0.5149$	confinement factor between stripes
$\alpha_w = 30 \text{ cm}^{-1}$	surface absorption constant
$\alpha_{sr} = 10^8 \text{ cm s}^{-1}$	surface recombination constant

respective frequencies are not directly available. As it turns out, for efficient stabilization schemes, information on both spatial modes and frequency distribution is crucial. We therefore extended the traditional eigenmode analysis to complex input data pertaining to the spatially resolved optical field.

A. Complex Karhunen-Loève decomposition

The complex eigenmodes \mathbf{p}_n corresponding to transverse modes $p_n(x)$ of the optical field are obtained by solving the eigenvalue problem of the Hermitian covariance matrix

$$\mathbf{C} \mathbf{p}_n = \lambda_n \mathbf{p}_n,$$

where

$$C_{jk} = \frac{1}{T} \int_0^T E^*(x_j, t) E(x_k, t) dt, \quad j, k = 1, \dots, N_x,$$

where T and N_x denote the length of the time series and the number of transverse grid points, respectively. The real eigenvalues λ_n yield the relative importance of the complex eigenmodes \mathbf{p}_n , which form an orthonormal set

$$\sum_{k=1}^{N_x} p_m^*(x_k) p_n(x_k) = \delta_{mn}. \quad (3)$$

The time-varying modal amplitudes are also complex quantities. They govern the dynamics of the individual eigenmodes and are obtained according to

$$a_n(t) = \sum_{k=1}^{N_x} p_n^*(x_k) E(x_k, t). \quad (4)$$

It is the frequency spectra of these modal time series $a_n(t)$ that yield the oscillation frequencies of the complex eigenmodes and will later help us in establishing suitable conditions for achieving stabilizing feedback. From the eigen-

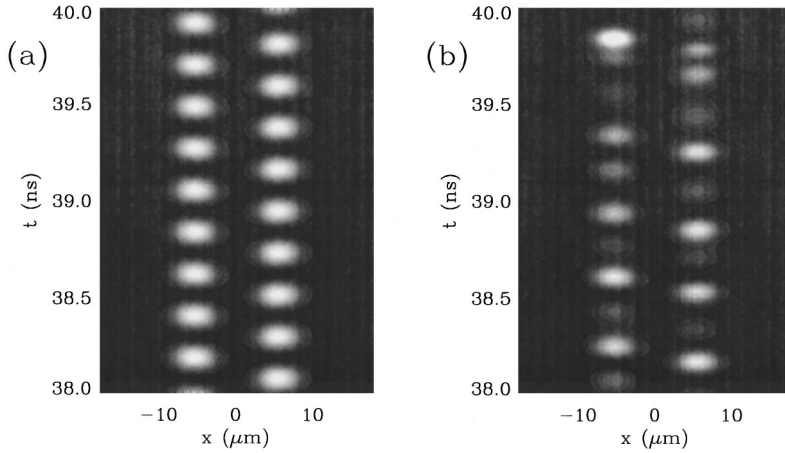


FIG. 1. Spatiotemporal dynamics of the intensity $I(x,t) = (1 - R_1) \epsilon_0 c / n_l |E(x,t)|^2$ for the two-stripe laser (a) in the periodic regime ($J = 45$ mA) and (b) in the chaotic regime ($J = 70$ mA), respectively, for intermediate diffusion $D_f = 4 \times 10^{-4}$ m²/s. Light shading corresponds to high-intensity values.

modes and expansion coefficients, the original complex optical field can be reconstructed by

$$E(x_k, t) = \sum_n a_n(t) p_n(x_k). \quad (5)$$

The same procedure can be carried out for the carrier density $N(x,t)$. Since $N(x,t)$ is real, its eigenmodes q_n and modal amplitudes $b_n(t)$ are real quantities. The reconstruction of the carrier density is obtained by

$$N(x_k, t) = \bar{N}(x_k) + \sum_n b_n(t) q_n(x_k), \quad (6)$$

where \bar{N} is the time-averaged carrier density profile.

B. Mode projection

The eigenmodes obtained from complex KLD can be used as an orthonormal basis for mode projection, in analogy to the Galerkin procedure. Thus the set of PDEs (1) and (2) can be transformed into a set of ODEs. To this end, the eigenmode decompositions of the optical field and the carrier density, i.e., Eqs. (5) and (6), are inserted into the PDEs. A set of ODEs for the modal amplitudes a_n and b_n is obtained by multiplying Eq. (1) with p_n^* and Eq. (2) with q_n and integrating over x . We make use of this approach in Sec. IV C in order to perform linear stability analysis.

IV. STABILIZATION OF CHAOTIC LASER ARRAYS

Depending on the separation between the laser stripes, semiconductor laser arrays are strongly, moderately, or weakly coupled [9,20]. In the regime of strong coupling (small separation between the lasers) the dynamical behavior is strongly dependent on the amount of external pumping via the electrical current. With increasing pump current, spatiotemporal instabilities arise in multistripe lasers due to the nonlinear interaction of multiple transverse modes. Not surprisingly, the higher the number of transversely coupled laser stripes, the larger the spatiotemporal complexity. The basic effects, however, can already be demonstrated with the simplest laser array, the two-stripe laser. Therefore, we start our discussion with this simple array. We then enlarge the configurations to three and five transversely coupled laser stripes.

A. Free-running two-stripe laser

For low values of the pump current, the two-stripe laser operates in a steady state of coherent light emission with one single transverse mode. However, when we increase the pump current above a critical threshold value J_c , an instability leading to spontaneous periodic intensity pulsations sets in. Several dynamical regimes with alternating pulsations in the two stripes are observed. A further increase of the current drives the laser into a both spatially and temporally irregular regime (Fig. 1). It is found that the value of J_c strongly varies with the amount of charge carrier diffusion, which is quite significant in semiconductor lasers.

Plotting the dependence of the total output power on the amount of applied pumping current represents a frequently used way of characterizing the operation conditions of semiconductor lasers. With the two-stripe laser being in the time-dependent regimes, single-mode operation in the fundamental mode is found to exist as an unstable solution. In Fig. 2 we plot the spatially averaged intensity emitted in this state versus the pump current applied to the laser (solid curves). The dashed curves represent the corresponding time-dependent regimes (periodic pulsing and chaos, respectively) which start at the critical current value J_c . In these regimes the laser system seems to have entered an operation condition that more effectively transforms inversion into output intensity: The output-intensity (both temporally and spatially averaged) is slightly larger than in the steady-state regime. For $J > J_c$, the steady state (solid lines) was obtained by the

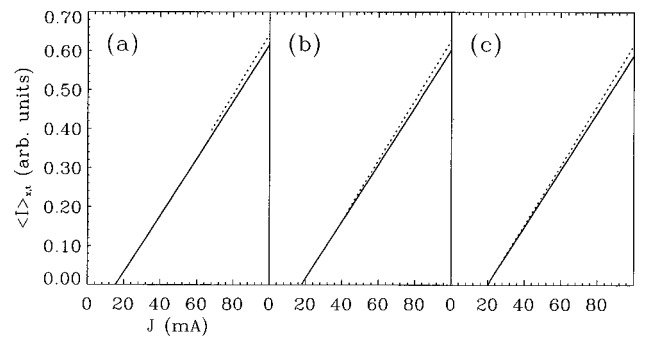


FIG. 2. Spatially and temporally averaged intensity for steady-state operation in a single transverse mode (solid line) and time-dependent regimes (dashed line) shown for three values of the carrier diffusion constant: (a) $D_f = 1 \times 10^{-4}$, (b) 4×10^{-4} , and (c) 8×10^{-4} m²/s.

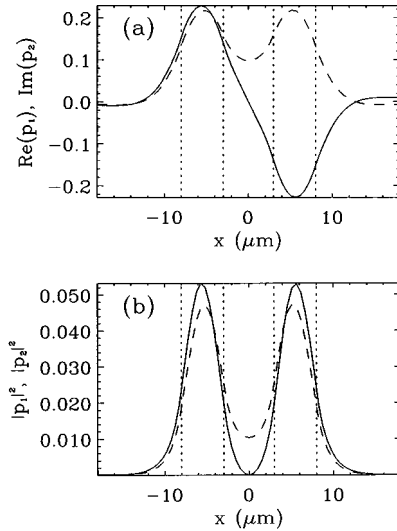


FIG. 3. Eigenmodes $p_1(x), p_2(x)$ for the two-stripe laser: (a) real part of the first eigenmode (solid line) and imaginary part of the second eigenmode (dashed line) and (b) “intensities,” i.e., squared moduli of the eigenmodes. The vertical lines indicate the locations of the laser stripes.

stabilization technique explained below. Remarkably, it is the continuation of the lines for $J < J_c$ where the laser is intrinsically stable. In the figure we show three curves for the case of low, intermediate, and high carrier diffusion. The larger the diffusion, the smaller the critical current value J_c .

Eigenmode analysis reveals that the spatiotemporal dynamics is governed by the two eigenmodes shown in Fig. 3. Here and in the following we plot the real (imaginary) part of the complex spatial profile, whenever it dominates over the imaginary (real) part. The first antisymmetric mode, which will be referred to as the fundamental mode, represents a mode where the two adjacent laser stripes oscillate with opposite phase. This mode represents the “natural” operation condition of stable transversely coupled laser arrays [21].

Due to the antisymmetric shape of the fundamental mode, its modulus is vanishing in the center of the gap separating the laser stripes. The second eigenmode is symmetric with respect to the two lasers; the time-dependent expansion coefficients associated with it represent in-phase oscillation of the stripes. In contrast to the antisymmetric mode, its modulus is clearly nonvanishing in the center of the gap. Therefore, the symmetric eigenmode can profit from the charge carriers diffusing towards the gap more than the fundamental mode. This effect becomes more and more important as the pump current increases, until at the critical current value the symmetric mode becomes involved in the dynamics. In the above-mentioned periodic regime, it coexists with the fundamental mode, leading to transverse mode beating. This beating generates the periodic intensity pulsations, whose frequency equals the difference between the mode frequencies. For high currents, there is mode competition rather than coexistence, which leads to chaotic behavior. The frequencies $\Omega_{1,2}$ pertaining to the first and second eigenmodes are obtained via the corresponding frequency spectra of the time series $a_{1,2}(t)$ (Fig. 4). In the periodic regime, the frequencies emerge as sharp lines, while in the chaotic regime the peaks are considerably broadened.

B. Stabilization by delayed optical feedback

Using the frequencies $\Omega_{1,2}$ of the transverse optical eigenmodes, we are able to establish a destructive interference condition in the symmetric mode in order to reobtain steady-state operation in the fundamental transverse mode. The influence of interference between external cavity modes and transverse modes was also considered in [10] in the case of a broad-area laser. In a steady-state condition, we can easily realize the effects of the delay term. Imagine the complex equation (1) for $E = R e^{i\theta}$ to be written as two real equations for amplitude R and phase $\theta = \omega t$. Then the delay term produces a contribution $\gamma_R R(x) \cos(\Phi - \omega\tau)$ in the amplitude equation, while a term $\gamma_R \sin(\Phi - \omega\tau)$ arises in the equation

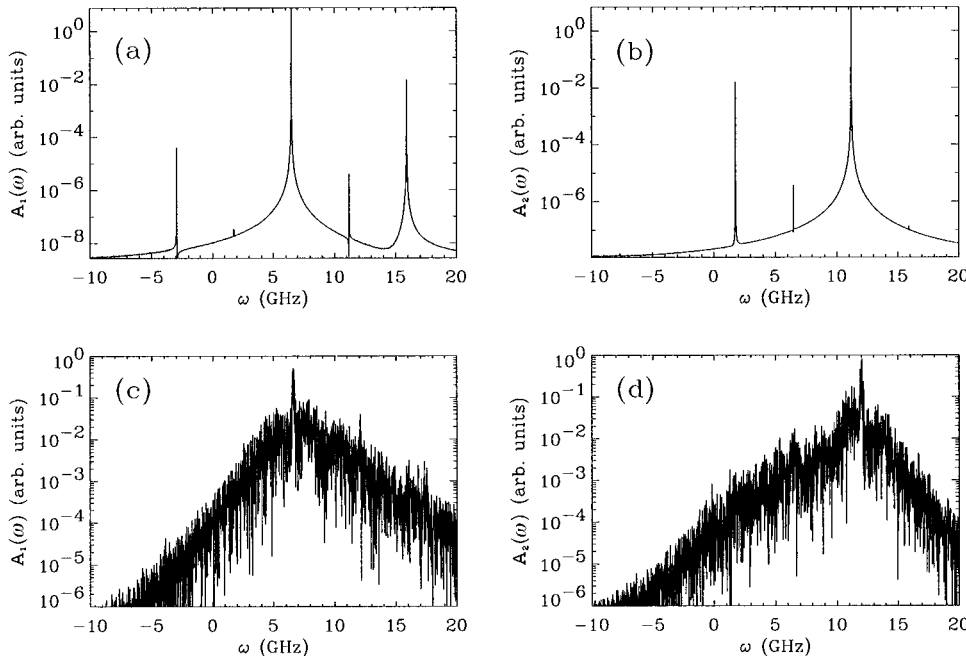


FIG. 4. Frequency spectra $A_1(\omega)$ and $A_2(\omega)$ of the time-varying modal amplitudes $a_1(t)$ and $a_2(t)$, respectively, pertaining to the two eigenmodes: (a) and (b) periodic regime ($J=45$ mA) and (c) and (d) chaos ($J=70$ mA).

for the phase. This means that there is a contribution to the gain of strength γ_R times a cosine dependence on the overall phase $\Psi = \Phi - \omega\tau$ that governs the interference condition. The contribution in the phase equation amounts to a frequency shift depending on γ_R and Ψ .

The contribution of delayed optical feedback to the gain can be graphically interpreted as the presence of a cosine-shaped filter in the frequency domain, which, for appropriately chosen feedback parameters τ and Φ , can cause destructive interference for light of a particular frequency. This effect can be used to provide damping in a transverse mode oscillating at that frequency.

Let ω_1 be the frequency of the fundamental mode and ω_2 that of the mode that we aim to suppress. The two parameters τ and Φ permit us to set up the two interference conditions

$$\Phi - \omega_2\tau = (n + \frac{1}{2}), \quad (7)$$

$$\Phi - \omega_1\tau = m, \quad n, m = 0, \pm 1, \pm 2 \dots \quad (8)$$

(here and in the following all phases are written in units of 2π). Equation (7) represents destructive interference in the transverse mode to be suppressed, while Eq. (8) describes constructive interference in the fundamental transverse mode, which seems to be a natural choice. Then τ and Φ are determined by

$$\tau = \frac{1}{2(\omega_2 - \omega_1)}, \quad (9)$$

$$\Phi = \omega_1\tau, \quad (10)$$

where the integers n and m were chosen such that the two frequencies for which the interference conditions are provided correspond to adjacent extrema of the cosine filter.

For a chaotic two-stripe laser with $J = 80$ mA, $D_f = 4.0 \times 10^{-4}$ m²/s (which is well within the chaotic range) we obtain the modal frequencies $\Omega_1 = 6.3$ GHz and $\Omega_2 = 12.1$ GHz. Identifying $\Omega_{1,2}$ with $\omega_{1,2}$ from Eqs. (9) and (10) then yields the values $\tau = 0.0862$ ns and $\Phi = 0.543$. With these parameters employed we indeed obtain stable cw operation in the fundamental antisymmetric mode. The stabilizing effect of delayed optical feedback is demonstrated in Fig. 5. For $t < t_0 = 20$ ns, $\gamma_R = 4 \times 10^{-2}$ and $\tau = \phi = 0$; for $t > t_0$, τ and Φ are set to the above values. After the chaotic interval, the symmetric eigenmode is quickly damped to zero, while the antisymmetric eigenmode approaches cw emission via damped relaxation oscillations. When stabilization is achieved and there is exactly constructive interference, the original system of equations, i.e., without delayed feedback, is effectively recovered. In this case, only one mode, for which $\Psi = 0$, exists. Thus the delay term in the phase equation is zero and the delay term in the amplitude equation reduces to a slightly enhanced reflectivity (γ_R). In this sense, our procedure bears some analogy to genuine schemes of controlling chaos where, upon successful control, the controlling force vanishes [5,22,23].

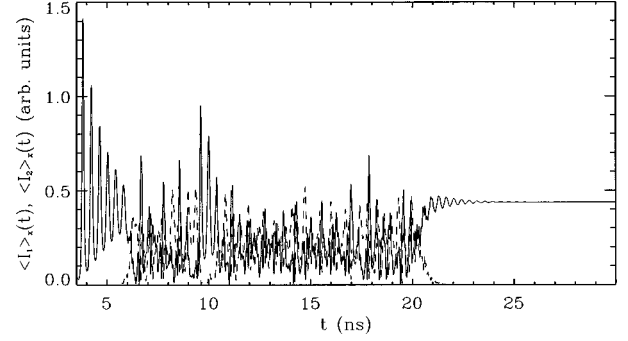


FIG. 5. Time series of the transversely averaged intensities $\langle I_1 \rangle_x(t), \langle I_2 \rangle_x(t)$ pertaining to the two eigenmodes (solid line, fundamental mode; dashed line, symmetric mode). Stabilization of the antisymmetric fundamental transverse mode is achieved after switching on time delay at $t_0 = 20$ ns. For $t < t_0$, $\gamma_R = 4 \times 10^{-2}$, and $\tau = \Phi = 0$; for $t > t_0$, $\gamma_R = 4 \times 10^{-2}$, $\tau = 0.0862$ ns, and $\Phi = 0.543$.

C. Robustness of stabilization: Numerical and analytical results

In order to give an idea of the parameter range where stabilization is possible, we consider deviations from the destructive interference condition while preserving constructive interference in the fundamental mode. To this end, we introduce a frequency mismatch $\delta\omega = \omega_2 - \Omega_2$ between the frequency where destructive interference happens and the frequency of the symmetric eigenmode. We then determine the range in $\delta\omega$ where stabilization persists in dependence of the feedback strength γ_R . We perform a linear stability analysis on the basis of the nonlinear eigenmodes in order to obtain a comparison between numerical and analytical results. To this end, we use the set of ODEs obtained by mode projection onto the eigenmodes (cf. Sec. III B). The following set of linearized ODEs describes the growth of perturbations of the modal amplitudes pertaining to the relevant eigenmodes (e_1 and e_2 for the optical field and n_1 and n_2 for the carrier density):

$$\begin{aligned} \dot{e}_1 = & \left(-\gamma_E - i\bar{\omega}_0 + i \int p_1^* \eta(x) p_1 dx + i D_p \int p_1^* \partial_x^2 p_1 dx \right) e_1 \\ & + \bar{\gamma}_R e^{i(\Phi - \bar{\omega}_0\tau)} e_1(t - \tau) + e_{1a} \int p_1^* \Gamma(x) [r\bar{N}(x) - N_0] \\ & \times p_1 dx + n_1 e_{0a} \int p_1^* \Gamma(x) \bar{r} q_1 p_1 dx, \\ \dot{e}_2 = & \left(-\gamma_E - i\bar{\omega}_0 + i \int p_2^* \eta(x) p_2 dx + i D_p \int p_2^* \partial_x^2 p_2 dx \right) e_2 \\ & + \bar{\gamma}_R e^{i(\Phi - \bar{\omega}_0\tau)} e_2(t - \tau) + e_{2a} \int p_2^* \Gamma(x) [r\bar{N}(x) - N_0] \\ & \times p_2 dx + n_2 e_{0a} \int p_2^* \Gamma(x) \bar{r} q_2 p_1 dx, \\ \dot{n}_1 = & \left(-\gamma_{nr} + D_f \int q_1 \partial_x^2 q_1 dx \right) n_1 - e_0 (e_1 + e_1^*) a' \\ & \times \int q_1 [\bar{N}(x) - N_0] |p_1|^2 dx - n_1 |e_0|^2 a' \int q_1^2 |p_1|^2 dx, \end{aligned}$$

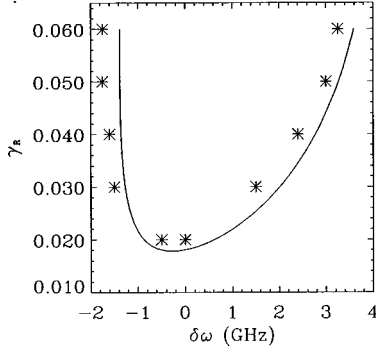


FIG. 6. Range of frequency mismatch $\delta\omega$, where stabilization is achieved for the two-stripe laser, versus the feedback strength γ_R ($J=80$ mA and $D_f=4\times 10^{-4}$ m²/s) (symbols, numerical simulation; solid curve, linear stability analysis).

$$\begin{aligned} \dot{n}_2 = & \left(-\gamma_{nr} + D_f \int q_2 \partial_x^2 q_2 dx \right) n_2 - a' \int q_2 [\bar{N}(x) - N_0] \\ & \times e_0 (e_2 p_1^* p_2 + e_2^* p_1 p_2^*) dx - n_2 |e_0|^2 a' \\ & \times \int q_2^2 |p_1|^2 dx, \end{aligned}$$

where $\bar{r} = 1 - i\alpha$, $\bar{\gamma}_R = (c/2n_1L)\gamma_R$, and $a' = (2\epsilon_0 c/\hbar\omega_0 n_1)a$ have been used.

In this analysis, the symmetric field mode is considered as a perturbation to the steady-state operation in the fundamental antisymmetric field mode. The latter is characterized by the field profile $e_0 p_1 \exp(i\bar{\omega}_0 t)$ and the carrier density profile $\bar{N}(x)$, respectively. These quantities were obtained by solving the steady-state equations. Since delayed feedback is involved, the growth of the perturbation is described by a transcendental eigenvalue equation, which has to be solved numerically. We achieve good agreement with the results of the numerical integration. In Fig. 6 a curve is shown that separates the stable from the unstable parameter region for the case of intermediate diffusion $D_f = 4.0 \times 10^{-4}$ m²/s. The symbols represent results from numerical simulations, while the solid curve was obtained by linear stability analysis. This figure shows that a minimum feedback strength is required in order to achieve stabilization. Above this value, stabilization persists in a considerable range of $\delta\omega$, which increases with γ_R .

The small displacement of the curves with respect to $\delta\omega$ in Fig. 6 is due to the fact that the frequency Ω_2 was determined from spectra of the chaotic regimes. In that case, where the symmetric mode is fully developed, the average carrier density profile is appreciably modified due to saturation. This causes a shift in frequency with respect to the situation considered in linear stability analysis, where the symmetric mode is only a small perturbation.

We observe two ways in which stabilization may break down, depending on whether the curve in Fig. 6 is crossed on the left or on the right branch. When the left branch is crossed for decreasing values of $\delta\omega$, the symmetric mode retains a finite amplitude leading to the periodic pulsations shown in Fig. 1. When the right branch is crossed for increasing values of $\delta\omega$, we observe an intermittent regime, where the symmetric mode appears in chaotic bursts.

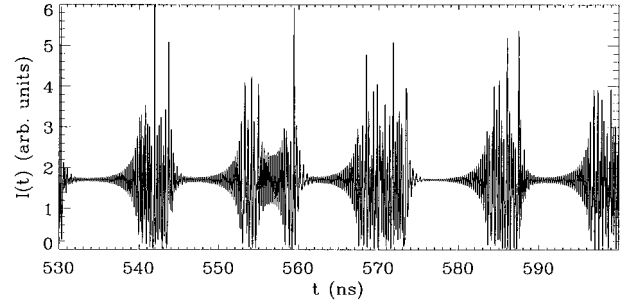


FIG. 7. Representative time series of the intensity in the center of a stripe within the intermittency range ($J=80$ mA, $D_f=8\times 10^{-4}$ m²/s, $\gamma_R=4\times 10^{-2}$, $\tau=0.0794$ ns, $\Phi=0.556$).

An example for the time series of the intensity taken in the center of a laser stripe is shown in Fig. 7 for the case of strong diffusion ($D_f=8.0\times 10^{-4}$ m²/s). A power-law scaling with an exponent equal to -1 is obtained, which could be a signature of type-II intermittency (Fig. 8). Indeed, Fig. 7 suggests a destabilization via a Hopf bifurcation. The same scaling behavior is obtained for various values of γ_R and D_f .

D. Three- and five-stripe laser arrays

Eigenmode analysis of multistripe lasers yields that the maximum number of relevant eigenmodes in the complex spatiotemporal regimes is equal to the number of stripes. Thus, in principle, several transverse modes have to be suppressed in order to stabilize laser arrays with more than two stripes. In the three-stripe laser, one fundamental plus two additional eigenmodes arise, which come into play in the time-dependent regimes (Fig. 9). Again, the fundamental mode is an out-of-phase eigenmode. The second eigenmode is symmetric and is localized at the inner stripe, while the third eigenmode is antisymmetric, being localized at the outer stripes. The second eigenmode has a comparatively large amplitude within the two gaps. This suggests that this mode is responsible for destabilization for high pump currents, in analogy to the findings for the two-stripe laser.

In analogy to the two-stripe laser case, the frequencies of the eigenmodes are obtained from the frequency spectra of their respective time series $a_1(t)$, $a_2(t)$, and $a_3(t)$ (Fig. 10).

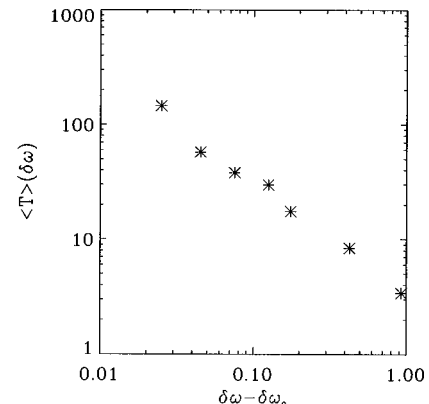


FIG. 8. Power-law scaling of the mean laminar lengths $\langle T \rangle$ versus the frequency mismatch $\delta\omega$, yielding an exponent -0.98 ± 0.05 .

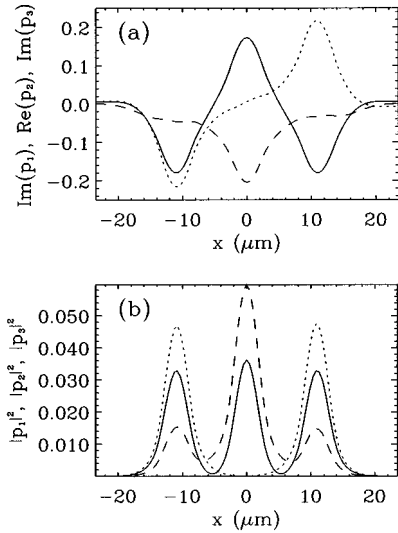


FIG. 9. (a) Eigenmodes $p_1, \dots, p_3(x)$ for the three-stripe laser and (b) their respective intensities, i.e., squared moduli. The solid, dashed, and dotted curves are referred to as the fundamental, the second, and the third eigenmode, respectively.

It turns out that the choice $\omega_1 = \Omega_1$, $\omega_2 = \Omega_2$, i.e., suppression of the second mode, leads to stable cw operation in the fundamental mode via suppression of the higher modes. Even in the case of the five-stripe array, where four relevant transverse modes exist in addition to the fundamental mode, stabilization of the fundamental mode can be achieved. An example where the five-stripe laser is brought from a state of spatiotemporal chaos to cw operation is shown in Fig. 11. However, the criteria with respect to the way how to choose

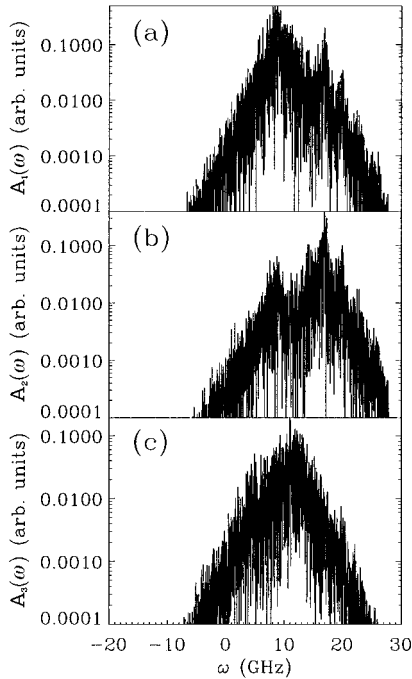


FIG. 10. Frequency spectra (a) $A_1(\omega)$, (b) $A_2(\omega)$, and (c) $A_3(\omega)$ of the time-varying modal amplitudes $a_1(t)$, $a_2(t)$, and $a_3(t)$, respectively, pertaining to the three eigenmodes of the three-stripe array for $J=100$ mA and $D_f=1 \times 10^{-4}$ m²/s, i.e., well within the chaotic range.

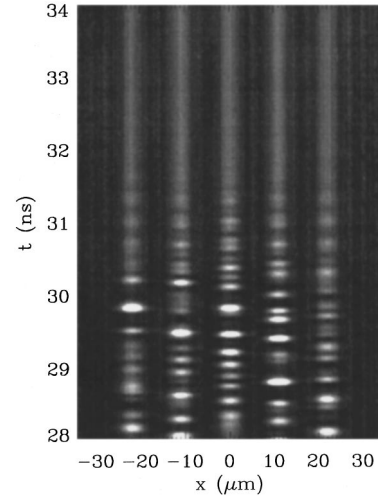


FIG. 11. Spatiotemporal dynamics of the five-stripe laser for $J=80$ mA, $\gamma_R=3 \times 10^{-2}$, $\tau=0.0877$ ns, and $\Phi=0.06$, where the time delay and feedback phase are switched from zero to the above values at $t=30$ ns.

ω_2 are not as obvious as in the case of the two- and three-stripe lasers. The mode to be suppressed varies with pump current and diffusion strength and in some cases the best results are obtained when ω_2 lies between two transverse mode frequencies. The fact that stabilization is still possible could be plausible if the successive transverse modes are nonlinearly coupled in a cascadelike fashion. Then damping of particular modes could cause the suppression of the whole cascade of modes.

V. CONCLUSION

We have demonstrated that multistripe laser arrays that exhibit spatiotemporal chaos already at moderate pumping can be stabilized by means of tailored delayed optical feedback. An appropriate choice of the interference conditions determined by the delay time and the feedback phase leads to stabilization of the fundamental out-of-phase array modes via suppression of the destabilizing transverse modes. In order to achieve the relevant feedback conditions, information about the frequencies of the transverse modes of the complex optical field were obtained by means of generalized complex eigenmode analysis.

The results and the stabilization scheme presented bear remarkable analogies to the characteristic methods in the field of chaos control. First, the single-mode operation in the fundamental transverse mode corresponds to an unstable solution that nevertheless exists also in the spatiotemporally chaotic domain. Second, the mode equations effectively reduce to the original system without feedback in the stabilized case, as explained in the text. In the case of the two-stripe laser, we found that, as feedback parameters are moved outside the stabilization range, stabilization breaks down either by the formation of periodic pulsing due to coexistence of the transverse mode to be suppressed or by intermittent appearance of that mode. In the latter case, we found a power-law scaling, which could originate from type-II intermittency. Stabilization was demonstrated also in cases, where several transverse modes have to be suppressed, in particular for the three-stripe and the five-stripe laser array.

- [1] R. Lang and K. Kobayashi, IEEE J. Quantum Electron. **QE-16**, 347 (1980).
- [2] Y. Cho and T. Umeda, Opt. Commun. **59**, 131 (1986).
- [3] J. Mørk, B. Tromborg, and J. Mark, IEEE J. Quantum Electron. **28**, 93 (1992).
- [4] D. Lenstra, B. H. Verbeek, and A. J. den Boef, IEEE J. Quantum Electron. **QE-21**, 674 (1985).
- [5] C. Simmendinger and O. Hess, Phys. Lett. A **216**, 97 (1996).
- [6] M. E. Bleich, D. Hochheiser, J. V. Moloney, and J. E. S. Socolar, Phys. Rev. E **55**, 2119 (1997).
- [7] H. Adachihara, O. Hess, R. Indik, and J. V. Moloney, J. Opt. Soc. Am. B **10**, 497 (1993).
- [8] H. Adachihara, O. Hess, E. Abraham, and J. V. Moloney, J. Opt. Soc. Am. B **10**, 658 (1993).
- [9] O. Hess and T. Kuhn, Prog. Quantum Electron. **20**, 84 (1996).
- [10] J. Martín-Regalado, S. Balle, and N. B. Abraham, IEEE J. Quantum Electron. **32**, 257 (1996).
- [11] O. Hess and E. Schöll, Physica D **70**, 165 (1994).
- [12] I. Fischer, O. Hess, W. Elsässer, and E. Göbel, Europhys. Lett. **35**, 579 (1996).
- [13] M. Münkler, F. Kaiser, and O. Hess, Phys. Lett. A **222**, 67 (1996).
- [14] J. Martín-Regalado, G. H. M. van Tartwijk, S. Balle, and M. San Miguel, Phys. Rev. A **54**, 5386 (1996).
- [15] G. P. Agrawal and N. K. Dutta, *Long-Wavelength Semiconductor Lasers* (Van Nostrand Reinhold, New York, 1986).
- [16] O. Hess, *Spatio-Temporal Dynamics of Semiconductor Lasers* (Wissenschaft und Technik-Verlag, Berlin, 1993).
- [17] O. Hess, Chaos Solitons Fractals **4**, 1597 (1994).
- [18] D. Merbach, O. Hess, H. Herzel, and E. Schöll, Phys. Rev. E **52**, 1571 (1995).
- [19] D. R. Korwan and G. Indebetouw, J. Opt. Soc. Am. B **13**, 1473 (1996).
- [20] S. S. Wang and H. G. Winful, Appl. Phys. Lett. **52**, 1774 (1988); H. G. Winful and S. S. Wang, *ibid.* **53**, 1894 (1988).
- [21] H. F. Hofmann and O. Hess, Quantum Semiclass. Opt. (to be published).
- [22] E. Ott, C. Grebogi, and J. A. Yorke, Phys. Rev. Lett. **64**, 1196 (1990).
- [23] K. Pyragas, Phys. Lett. A **170**, 421 (1992).